



Photocatalytic Activity of Zr Doped ZnO and Its Morphology

Arumugam Vijayabalan^{1, 2, *}, Ayyanar Sivakumar², Nadarajan Suresh Babu³,
Arumugam Amalorpavadoss²

¹Department of Chemistry, King Nandhivarman College of Arts and Science, Thellar, Kanchipuram, India

²Department of Chemistry, St. Joseph's College of Arts and Science (Autonomous), Cuddalore, India

³Department of Chemistry, Government College of Engineering, Thanjavur, India

Email address:

vijayabalanchem@gmail.com (A. Vijayabalan)

*Corresponding author

To cite this article:

Arumugam Vijayabalan, Ayyanar Sivakumar, Nadarajan Suresh Babu, Arumugam Amalorpavadoss. Photocatalytic Activity of Zr Doped ZnO and its Morphology. *International Journal of Bioorganic Chemistry*. Vol. 4, No. 1, 2019, pp. 14-18. doi: 10.11648/j.ijbc.20190401.13

Received: February 3, 2019; Accepted: March 8, 2019; Published: March 30, 2019

Abstract: Doped ZnO with Zr has been obtained by sol-gel method and characterized by powder X-ray diffraction, energy dispersive X-ray spectrum, Scanning electron micrographs, and UV-visible diffuse reflectance and photoluminescence spectroscopy. Powder XRD shows that synthesized Zr doped ZnO has hexagonal wurtzite structure and high crystallinity, DRS reveals that wavelength are shifted from UV region to visible region when Zr doping. PL spectra clearly reveal that the recombinations of electron-hole pair in ZnO are suppressed by Zr doping. Zr-doping enhances the photocatalytic degradation of methylene blue dye than ZnO under visible light.

Keywords: Sol-gel Method, Zr-ZnO, Visible Light, Methylene Blue Dye

1. Introduction

In recent years, many researchers are discovered the new and modified semiconductor materials and application of these materials is cleaning the toxic effluents. ZnO photocatalyst is 3.2 eV and high photoactivity in UV spectrum [1]. ZnO photocatalyst are used in luminescence, optics, optoelectronics, sensors, actuators, energy, biomedical sciences, and spintronics. ZnO has been used as a photocatalyst, owing to its high activity, low cost and friendly environment. However, the problem of ZnO is the high recombination rate of electron-hole pair, resulting in low degradation efficiencies of the organic pollutants. To overcome these limitations, a number of strategies have been adopted to improve the charge separation efficiency and then enhance the photocatalytic activity of the catalyst such as the Semiconductors doping or hybridizing. ZnO modified with FeO semiconductor [2]. To study the influences of Zr-doped ZnO and nanosized ZrO₂ system structure and photocatalytic performance and ultrasoft pseudopotential method also influence ZnO structure [3-5]. Effect of Zr doping and Zr-Al co doping on the electrical and optical properties of ZnO [6, 7]. Report that the

grain size of Zr-doped ZnO is small and the surface area is high. Also within 0.2-1at% Zr-doping, the higher the doping amount is, the stronger the photocatalytic activity [8]. Utilized sol-gel method to study the influences of Zr-doping on ZnO photoelectric properties. The results showed that when Zr-doping fell in 0-5at%, the resistances of all the doping systems all were greater than that of pure ZnO. Moreover, when the doping amount was 3at%, the transmissivity of the doping system was the most ideal. Kim *et al.* to study the photoelectric property of Zr-doped ZnO system by using pulse laser deposition method [9]. The results indicate that the higher the oxygen pressure is, the greater the doping system resistance is and the higher the transmissivity. Many methods are reported as synthesize coupled metal oxides are photo-deposition method [10] solid state dispersion method [11] hydrothermal method [12] impregnation method [13, 10], sol-gel method [14], co-precipitation method [15-17] mechanical mixing method [18], flame spray pyrolysis [19] and microwave synthesis. [20].

The present paper reports the environmental friendly greener synthesis of novel Zr-doped ZnO using sol-gel synthesis and investigations on its photocatalytic activity

under visible light for the degradation of MB dye.

2. Materials and Methods

2.1. Materials

Zr(NO₃)₃(Loba-chemi), Zn(NO₃)₂(Loba-chemi), Methylene blue dye(Merck) and liquid ammonia(Qualigens) were used. Distilled water is used for the makeup solution.

2.2. Methods

Preparation of Zr-ZnO by Sol-gel method

To appropriate concentration of Zn (NO₃)₂ and Zr (NO₃)₃ solution was added under stirring. After 1:1 aqueous ammonia solution was added to reach a pH 9.5 under continuous stirring. The crystals were collected by filtration, dried and calcined at 500°C for 1 h in a muffle furnace fitted with a PID temperature controller. The heating rate was 10°C min⁻¹. The undoped ZnO crystals were synthesized by adopting the same procedure but without Zr(NO₃)₃. The chemicals used were of analytical grade and deionized distilled water was employed for the experiments.

2.3. Characterization Techniques

A PANalytical X'Pert PRO diffractometer with Cu Kα rays of 1.5406 Å was employed to record the powder X-ray diffractograms (XRD) of the samples at 40 kV and 30 mA with a scan rate of 0.04°s⁻¹ in a 2θ range of 10–75°. The morphologies of Zr-doped ZnO and ZnO synthesized by sol-gel method were assessed using a JSM6610 model scanning electron microscope (SEM) under vacuum mode. The energy dispersive X-ray (EDX) spectrum was obtained using the Oxford instruments attached to scanning electron microscope (SEM). The diffuse reflectance spectra were obtained with a PerkinElmer Lamda 35 spectrometer. A PerkinElmer LS 55 fluorescence spectrometer was used to record the photoluminescence (PL) spectra at room temperature.

2.4. Photocatalytic Activity

The visible light photocatalytic studies were made in an immersion type photo reactor equipped with a 150-W tungsten halogen lamp fitted into a double walled borosilicate immersion well of 40 mm outer diameter with inlet and outlet for circulation of K₂Cr₂O₇ solution. The 1N K₂Cr₂O₇ solution used removes 99 % of the UV light with wavelength between 320 and 400 nm and acts as a UV cutoff filter. After the addition of the catalyst to the dye solution, air was bubbled through the solution which kept the catalyst particles under suspension and at constant motion. The catalyst was separated after the illumination. The dye Methylene blue was analyzed spectrophotometrically at 656 nm.

3. Results and Discussion

3.1. Crystal Structure and Morphology

The energy dispersive X-ray diffraction spectrum of Zr-ZnO is shown in figure 1. It reveals that Zr, Zn and O

element. It is concluding that 1.83% Zr doped ZnO lattice. Figure 2. Shows that the scanning electron microscope image of Zr-ZnO particles. It shows that hexagonal structures of ZnO are destroyed with doped Zr³⁺ ion. It also confirms that doped ZnO as micron size.

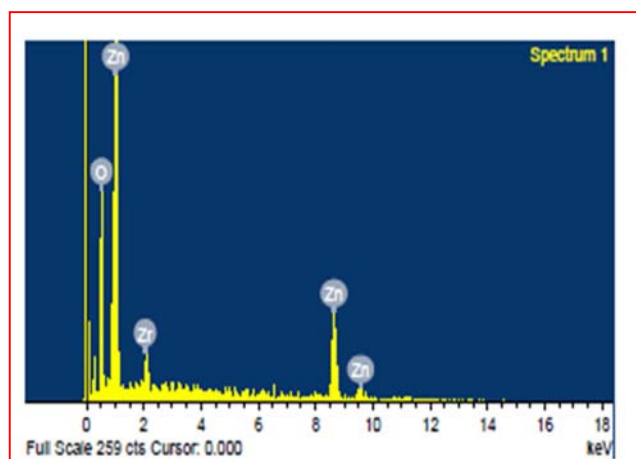


Figure 1. Energy dispersive X-ray spectrum of Zr-ZnO.

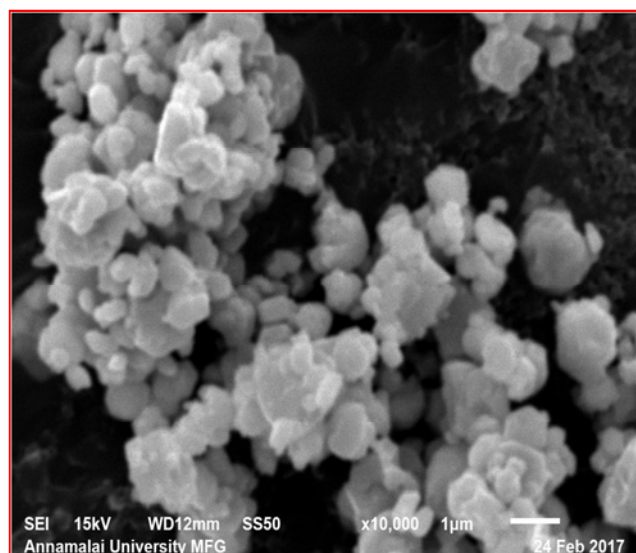


Figure 2. SEM images of Zr-ZnO.

The powder X-ray diffraction spectra of ZnO and Zr-ZnO are shown in figure 3. For bare ZnO, the diffraction peaks are located at 2θ=31.737, 34.379, 36.215, 47.484, 56.536, 62.777, 66.304, 67.868, and 69.009 are associated with [100], [002], [101], [102], [110], [103], [200], [112] and [201] planes respectively. This pattern has been indexed as hexagonal wurtzite phase of ZnO with lattice constants a=b=0.324nm and c=0.521 nm (JPCDS card number: 89-1397), and further it is also confirmed that the synthesized catalyst is free of impurities as it does not contain any characteristic XRD peaks other than ZnO peaks. Sol-gel synthesized Zr-ZnO diffraction pattern totally match with bare ZnO pattern. Further, the absence of cubic phase of ZrO₂ peak at 2θ value is 30.30, 35.40, 50.60, 59.8, 62.85° (JCPDS card no: 27-0997), monoclinic (JCPDS no 37-1484) and

tetragonal phase (JCPDS no: 86-0965) of ZrO_2 are absent in Zr-ZnO catalyst. Sharp diffraction peaks indicate that the samples have high crystallinity. The average particle size (D) is calculated by using the Debye-Scherrer's equation $D = 0.9\lambda/\beta\cos\theta$. Where, λ is the X-ray wavelength of 1.54 Å, β is the full-width at half maximum, θ is the Bragg's diffraction angle and surface area calculated by $S = 6/\rho D$, where S is the specific surface area, D is the average particle size and ρ is the material density. From the table-1, the crystal size of bare ZnO and Zr-ZnO are 10.06 and 12.16 nm corresponding surface area is 105.2 and 73.08 m^2g^{-1} respectively. It is also shows that the average particles size no change with Zr doped compare to bare ZnO.

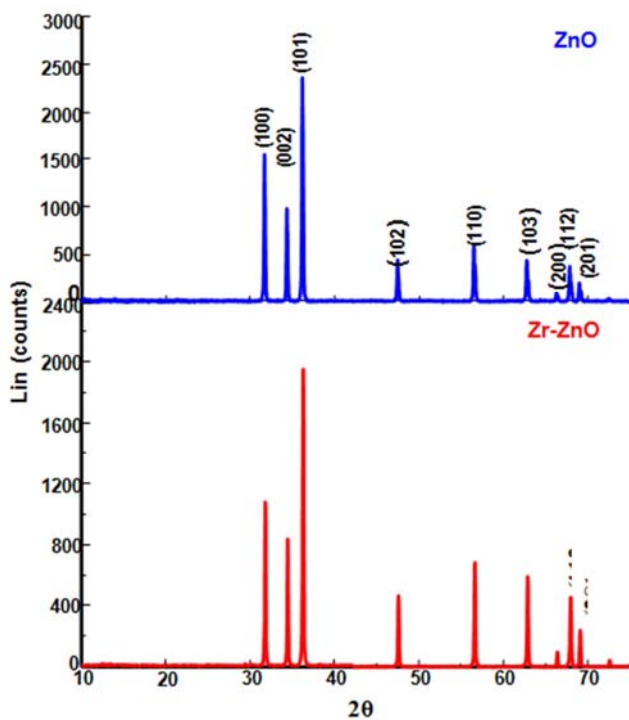


Figure 3. Powder X-ray diffraction spectrum of Zr-ZnO and ZnO.

Table 1. Crystal size (D) and Surface area (S) of ZnO and Zr- ZnO.

| Oxide | D , nm | S , m^2g^{-1} |
|--------|----------|-------------------|
| ZnO | 10.08 | 105.2 |
| Zr-ZnO | 12.16 | 73.08 |

3.2. Band Gap Energy

The diffuse reflectance spectrum of Zr-ZnO are shown in figure 4. In Zr-ZnO particles has higher absorption in visible region compare to bare ZnO (not shown in figure). To calculate the band gap energies of Zr-ZnO catalysts, UV-vis spectra in the diffuse reflectance mode (R) were transformed to the Kubelka-Munk function $F(R)$ to separate the extent of light absorption from scattering. The direct band gap energies of Zr-ZnO catalysts was obtained from the plot of the modified Kubelka-Munk function $[F(R)E]^2.0$ versus the energy of the absorbed light E are shown in figure 5 The direct band gap energy of Zr-ZnO particles is 3.02eV.

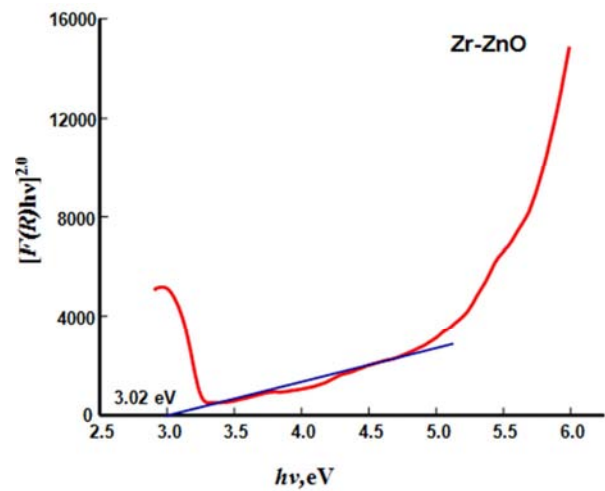


Figure 4. Tauc plot for direct band gap energy of Zr-ZnO.

3.3. Photoluminescence

The photoluminescence (PL) spectra of the bare ZnO and Zr- ZnO, are shown in figure 5 and figure 6 respectively. Photoluminescence occurs due to the recombination of electron-hole pair in the semiconductor. The loading Zr with ZnO does not shift the emission of ZnO, but the intensity of PL emission decreases when compared to bare ZnO. The trapping of photogenerated electron by Zr reduces the electron-hole recombination leading to the decrease of PL emission. This decrease in the rate of electron-hole recombination enhanced the photocatalytic activity of ZnO.

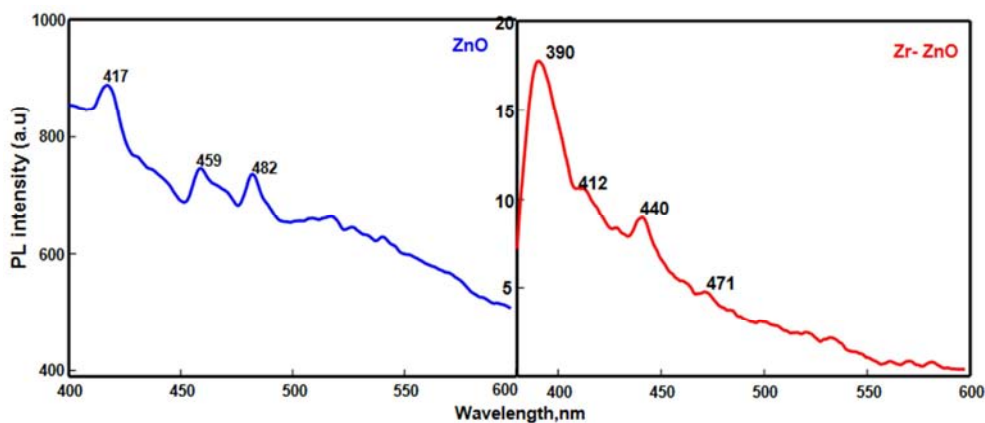


Figure 5. Photoluminescence spectra of ZnO and Zr doped ZnO.

3.4. Dye Degradation

The temporal profiles degradation of methylene blue dye under visible light is shown in figure 6. It is noted that the 58% (remaining 4.5ppm dye solution) degradation is observed for Zr-ZnO in 180 min. whereas ZnO degrade 41%(remaining 6.2 ppm dye solution) in 180 min. This might be due to trapping photo-excited electrons at conduction band by decreasing the electron-hole recombination as a consequence of Zr dopant into ZnO environment. Doping has regulated the degradation occurred by exhibiting the highest photo catalytic degradation efficiency in methylene blue dye This is because the incorporated Zr atom acts as electron traps by suppressing the recombination of photo-generated holes and electrons.

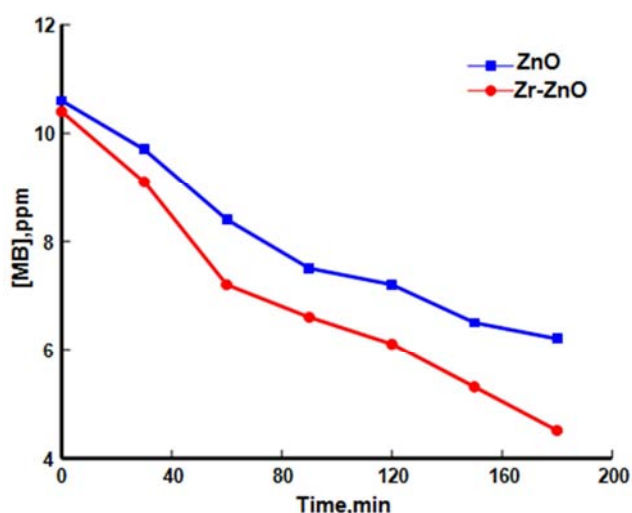


Figure 6. Temporal profiles of degradation of methylene blue dye under Visible light.

4. Conclusions

The $\approx 2\%$ Zr doped ZnO was prepared by sol-gel method. XRD reveals that prepared Zr doped ZnO as hexagonal wurtzite structure and absence of Zr^{3+} ion peak in ZnO crystals. SEM images shows the prepared doped ZnO micron in size and destroy the hexagonal wurtzite structure of ZnO with addition of Zr^{3+} ion, EDX confirms the presence of Zr^{3+} ion in ZnO crystals, DRS spectrum confirms the direct band gap energy of Zr doped ZnO is 3.02eV. Zr^{3+} ion does not shift the emission of ZnO, but the intensity of PL emission decreases when compared to bare ZnO. Zr doped ZnO is more enhanced photocatalytic degradation of methylene blue dye than bare ZnO under visible light.

References

- [1] S. M. Lama, J. A. Queka, J. C. Sin. Mechanistic investigation of visible light responsive Ag/ZnO micro/nanoflowers for enhanced photocatalytic performance and antibacterial activity, *J. of Photochem. Photobiol., A: Chem.*, vol. 353, pp. 171–184, 2018.
- [2] O. Bechambi, M. Chalbi, W. Najjara, and S. Sayadi., Photocatalytic activity of ZnO doped with Ag on the degradation of endocrine disrupting under UV irradiation and the investigation of its antibacterial activity, *applied surface science*, <http://dx.doi.org/doi:10.1016/j.apsusc.2015.03.049>.
- [3] S. N. Basahel, Tarek T Ali, M. Mokhtar, and K. Narasimharao., Influence of crystal structure of nanosized ZrO_2 on photocatalytic degradation of methyl orange, *Nano. Res. Lett.*, DOI 10.1186/s11671-015-0780-z.
- [4] N. C. S. Selvam, J. J. Vijaya, L. J. Kennedy, Effects of Morphology and Zr Doping on Structural, Optical, and Photocatalytic Properties of ZnO Nanostructures, *Ind. Eng. Chem. Res.* Vol. 51, pp. 16333, 2012.
- [5] F. G. Wang, M. S. Lv, Z. Y. Pang, T. L. Yang, Y. Dai, S. H. Han., Theoretical study of structural, optical and electrical properties of zirconium-doped zinc oxide, *Appl. Surf. Sci.* vol. 254, pp. 6983, 2008.
- [6] Q. Hou, C. Zhao, Z. Xu., Effect of Zr doping on the electrical and optical properties of ZnO, *Chem Phys. Lett.*, <http://dx.doi.org/10.1016/j.cplett.2016.06.075>.
- [7] J. H. Luo, Q. Liu, L. N Yang, Z. Z. Sun, Z. S. Li., First-principles study of electronic structure and optical properties of (Zr–Al)-codoped ZnO, *Comp. Mater. Sci.*, vol.82, pp. 70, 2014.
- [8] C. Y. Tsay, K. S. Fan., Optimization of Zr-doped ZnO thin films prepared by sol-gel method, *Mater. Trans.*, vol. 49, pp. 1900, 2008.
- [9] H. Kim, J. S. Horwitz, W. H. Kim, S. B. Qadri, Z. H. Kafafi., Anode material based on Zr-doped ZnO thin films for organic light-emitting diodes, *Appl. Phys. Lett.*, vol. 83, pp. 3809, 2003.
- [10] P. Sathishkumar, R. Sweena, W. Jerry, S. Anandan, Synthesis of CuO–ZnO nanophotocatalyst for visible light assisted degradation of a textile dye in aqueous solution, *J. Chem. Eng.*, vol. 171, pp. 136–140, 2011.
- [11] A. Kambur, G. S Pozan, I. Boz. Preparation, characterization and photocatalytic activity of TiO_2 – ZrO_2 binary oxide nanoparticles, *Appl. Catal. B: Environ.* vol. 115, pp. 149–158, 2012.
- [12] W. Liao, T. Zheng, P. Wang, S. Tu, W. Pan., Efficient microwave-assisted photocatalytic degradation of endocrine disruptordimethylphthalate over composite catalys ZrO_x/ZnO , *J. Environ. Sci.* vol. 22, pp. 1800–1806, 2010.
- [13] J. C. Tristao, F. Magalhaes, P. Corio, M. T. C. Sansiviero. Electronic characterization and photocatalytic properties of CdS/ TiO_2 semiconductor composite, *J. Photochem. Photobiol. A: Chem.*, vol. 181, pp. 152–157, 2006.
- [14] B. Neppolian, Wang, H. Yamashita, H. Choi., Synthesis and characterization of ZrO_2 – TiO_2 binary oxide semiconductor nanoparticles: application and interparticle electron transfer process, *Appl. Catal. A*, vol. 333, pp. 264–271, 2007.
- [15] H. Zou, Y. S Lin., Structural and surface chemical properties of sol-gel derived TiO_2 – ZrO_2 oxides, *Appl. Catal. A: Gen.*, vol. 265, pp. 35–42, 2004.
- [16] H. Wang, S. Baek, J. Lee, S. Lim. High photocatalytic activity of silver- loaded ZnO– SnO_2 coupled catalysts, *Chem. Eng. J.* vol. 146, pp. 355–361, 2009.

- [17] K. Vignesh., R. Priyanka., M. Rajarajan. A. Suganthi., Photo reduction of Cr (VI) in water using $\text{Bi}_2\text{O}_3\text{-ZrO}_2$ nanocomposite under visible light irradiation, *Mater. Sci. Eng. B*, vol. 178, pp 149–157, 2013.
- [18] W. Zheng. Z. Bingru. L. I. Fengting., A simple and cheap method for preparation of coupled ZrO_2/ZnO with high photocatalytic activities, *Front. Environ. Sci. Eng. China*. vol 1, pp. 454–458, 2007.
- [19] C. Chaisuk. A. Wehatoranawee. S. Preampiyawat. S. Netiphat. A. Shotipruk. J. Panpranot, B. Jongsomjit. O. Mekasuwandumrong. Preparation and characterization of $\text{CeO}_2/\text{TiO}_2$ nanoparticles by flame spray pyrolysis, *Ceram. Int.* vol. 37, pp. 1459–1463, 2011.
- [20] E. D. Sherly. J. Judith Vijaya. N. ClamentSagayaSelvam. L. JohnKennedy. Microwave assisted combustion synthesis of coupled ZnO-ZrO_2 nanoparticles and their role in the photocatalytic degradation of 2, 4-dichlorophenol, *Ceram. Inter.*, vol. 40, pp 5681–5691, 2014.